Chapter 15
Nanomaterials and Their Applications in Bioimaging

Ruma Rani, Khushboo Sethi, and Geeta Singh

Contents

R. Rani · K. Sethi
ICAR-National Research Centre on Equines, Hisar, India

G. Singh (✉)
Department of Biomedical Engineering, Deenbandhu Chhotu Ram University of Science and Technology, Sonipat, India
e-mail: geetasingh.bme@dcrustm.org

R. Prasad (ed.), *Plant Nanobionics*, Nanotechnology in the Life Sciences,
https://doi.org/10.1007/978-3-030-16379-2_15

15.1 Introduction

Nanomaterials have been widely studied by the researchers for their application in the area of nanomedicine for the diagnosis, monitoring, treatment, and prevention of disease. Change in the properties of nanomaterials compared to bulk materials occurs mainly because of large surface-area-to-volume ratio and dominance of quantum effects at nanoscale. These two effects enhance the properties such as reactivity, strength, electrical characteristics, optical characteristics, and magnetic characteristics and also in vivo behavior of nanomaterials. Moreover, in the field of chemistry, biotechnology, and biomedicine, nanomaterials have been used actively. Furthermore, biosensing, gene/drug delivery, bioimaging, multiplexed detection, and cancer chemotherapy have also been influenced from nanomaterial (Biju 2014). Recently, inorganic nanoparticles have attracted attention in the fields of imaging owing to their electronic, optical, magnetic properties and their inertness. The various abilities of nanomaterials allow one to use these for the detection of the structures and functioning of subcellular organelles and biomolecules. Moreover, they provide an emerging alternative for image-guided therapies in disease diagnosis and treatment of various diseases.

According to the perception of most people, 'imaging' is a kind of photography. But in scientific domain, it is far beyond this. Bioimaging is the visualization of biological processes in real time with less interference in life process and also gave output in the form of 3D (three-dimensional) images of any part of the body from outside. Various bioimaging techniques are available by which one can observe cells in tissues up to whole organism by using different sources of light, such as ultrasound, fluorescence, X-ray, electrons, magnetic resonance, and positrons. On the basis of the above source used, there are different bioimaging techniques such as magnetic resonance imaging (MRI), computed tomography (CT), positron emission tomography (PET), ultrasound, and fluorescence imaging that have been obliged to for disease diagnosis in clinical studies (Fig. 15.1). Out of the above said imaging techniques, MRI with the use of nanomaterials as contrast agents for in vivo imaging is the largest field of application (Li et al. 2015). Contrast agents are generally used in these bioimaging techniques in order to diagnose the organ or tissue of interest as well as identify healthy tissue from diseased tissue. The accurate diagnosis at the early stage of diseases is the need of hour that require a sensitive, specific, and high-quality imaging probes which can be possible with the following prerequisite qualities of the contrast agent:

- Stability of the agent in physiological environment with varying ionic strengths, pH, or temperature)
- Maintenance of colloidal solution with proper dispersion
- High retention time in bloodstream
- Proper imaging time and image contrast
- Longtime circulation in bloodstream after intravenous administration
- More biocompatibility of the agent
- Less cytotoxicity with systemic clearance

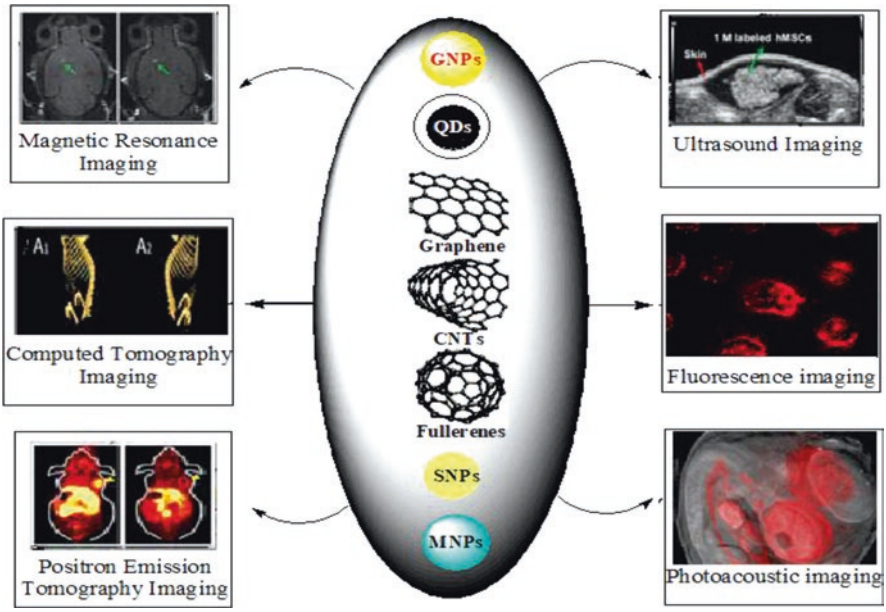

Fig. 15.1 Schematic representation of various imaging applications including magnetic resonance imaging (MRI), computed tomography (CT), positron emission tomography (PET), ultrasound imaging (USI), fluorescence imaging (FI), and photoacoustic imaging (PAI) with reference to different nanomaterials

Nanomaterial can be categorized into organic and inorganic nanomaterials that can be employed for imaging application. Due to ease in the synthesis and modification of inorganic nanomaterials, these novel designs and formulations are impacting conventional ones and show perspective employment in bioimaging (Cherukula et al. 2016). Among nanomaterials, gold nanoparticles, silica nanoparticles, magnetic nanoparticles, quantum dots, carbon nanotubes, fullerenes, and graphene have been used for imaging applications.

15.2 Nanomaterials for Bioimaging

15.2.1 Gold Nanoparticles

Gold nanoparticles (GNPs) are the most commonly used nanocarriers owing to their brilliant coloring, size, shape, and tunable surface plasmon properties which make them attractive for various applications such as sensing, diagnosis, catalysis, drug delivery, and bioimaging (Saha et al. 2012; Shi et al. 2012; Liang et al. 2015). The importance of colloidal gold was realized when monodispersed GNPs were prepared by the citrate reduction of gold ions. Schiffrin–Brust, in 1994, gave the most popular

synthetic method for GNPs with a biphasic approach by using a simple method and common reagents. In this method, gold ions were reduced by $NaBH_4$ in an aqueous phase; then, these were transferred to an organic phase with alkane thiol supplemented for the synthesis of thiol-protected gold nanoparticles (Brust et al. 1994). Afterward, Murphy et al. (2008) and Dreaden et al. (2012) gave GNP preparation method using seed-mediated growth having different kinds of size and shapes such as nanocubes, nanocages, and nanorods with satisfactory reproducibility. Templeton et al. (2000) synthesized GNPs with water dispersion characteristic by performing various ligand exchange reactions for the functionalization of terminal moiety on alkane thiol-protected GNPs. Their simple formulation and reactive surface allow for a variety of molecules to be attached which include drugs, targeting peptides or proteins, contrast agents, or other moieties. Different types of shapes like spheres, hollow shells, star shapes, rods, clusters, and cubes and size of particles ranging from 1 nm to over 100 nm have important effect on the optical properties of GNPs and their application (Mahan and Doiron 2018). For the first time, GNPs were investigated as an X-ray contrast agent by Hainfeld, who imaged the organs and vasculature of mice by injecting bare GNPs intravenously (Hainfeld et al. 2004, 2006). Nanomaterials shape also plays an important role in the application part like nanospheres, and nanorods of gold provide excellent contrasts in the dark-field optical and photothermal imaging of cells and tissues, whereas the nanoshells, nanospheres, nanorods, and nanocages are ideal for optical coherence tomography and photoacoustic imaging of deep tissues, circulatory systems, and lymph nodes (Biju 2014).

15.2.2 Silica Nanoparticles

Silica nanoparticles (SNPs) are another important group of inorganic delivery system. They are ideal candidates for bioapplications such as bioimaging/delivery applications owing to the straightforward, size-controllable morphologies, hydrophilic surface with biocompatibility, and ease of functionalization. Silica is accepted by FDA (US Food and Drug Administration) and has been widely used in cosmetics (Contado et al. 2013). Furthermore, Ow et al. (2005) reported that Cornell dots (commercial name) of SNPs encapsulating fluorescent dyes have also been evaluated as cancer-targeted imaging probes for stage I human clinical trial. The basis of silica nanoparticle preparation is based on the controlled hydrolysis of silyl ethers into silanols in the presence of ammonia in a mixture of water and alcohol followed by the condensation of silanols which results in the formation of 50–2000 nm silica particles. By varying the concentrations of silyl ether and alcohol, or the normal or reverse, one can control the size of SNPs (Trewyn et al. 2007). Mesoporous SNPs are prepared by the sol–gel process, involved in situ polymerization of silyl ethers and further more stabilized by surfactants in amphiphilic templates. Aggregation of SNPs can be avoided by optimizing the concentration of silyl ether or by the addition of various nonionic surfactants, polymers, triethanolamine, or propanetriol. Size can also be controlled by varying parameters like changing the pH of the

solution, solvent composition, and introduction of certain swelling agents. Thereafter, the amphiphilic templates can be removed by using different processes like solvent extraction, thermal decomposition, dialysis, or oxidation. Reactive functional groups can be added onto the SNP surface either at the time of preparation or after preparation (Wu et al. 2013). Modification of SNPs with surface functional groups such as primary or secondary amino, carboxyl, hydroxyl, alkyl halogen, or azide group is necessary for the conjugation of various biomolecules, contrast agents, and drug molecules to the surface as well as inside the pores of NPs. Moreover, hydrophilic nature of SNPs makes them one of the friendliest nanomaterials for biomedical applications such as drug and gene delivery, bioimaging, and therapy.

15.2.3 Magnetic Nanoparticles

Magnetic nanoparticles (MNPs) are made up of maghemite (Fe_2O_3) or magnetite (Fe_3O_4). Iron oxide materials are biodegradable, biocompatible, less toxic, and approved by FDA. MNPs possess superparamagnetism, as they are present in nanometric scale and smaller than the single domain limit. Moreover, in the absence of an external magnetic field, they have H_c (coercive field-minimum energy reverse the material net magnetization zero) and M_R (residual magnetization with no applied field) equal to zero, which make it a superparamagnetic and ideal candidate for bioapplications. MNPs have been widely used in various applications like multimodal imaging, targeted drug and gene delivery, hyperthermia for cancer treatment, biomedical separation, and tissue repair particularly owing to their unique superparamagnetic properties, tunable size as well as their conjugation with many biological and drug molecules (Liang et al. 2015). In general, there are several chemical methods for the synthesis of MNPs such as sol–gel, microemulsion, thermal decomposition, solvothermal hydrothermal protocols, electrochemical approaches, etc. (Laurent et al. 2008; Reddy et al. 2012). For targeted/therapeutic application of MNPs, one has to modify the organic shell surrounding the magnetic core, further giving rise to a water-soluble biocompatible product which can be further functionalized with chemically reactive groups. After modification of the organic shell for MNP attachment, NP surface can also be modified with the targeting moiety for targeted delivery. MRI, based on computer-assisted imaging within the human internal organs excited by radiofrequency waves under a gradient magnetic field, has become a useful diagnostic tool in medical science. MRI suffers from less sensitivity as well as inadequate spatial or temporal resolution. Therefore, MRI is combined with imaging techniques (MRI/PET, MRI/CT) for reducing their disadvantages. Lee et al. (2012) synthesized biocompatible Fe_3O_4–TaO_x core–shell NPs to achieve the benefits of two imaging techniques CT and MRI for imaging newly formed blood vessels in the tumors and tumor microenvironment, respectively.

15.2.4 Quantum Dots

Semiconductor quantum dots (QDs) are one of the most important QDs, whose size and shape can be accurately controlled by optimizing the time duration, temperature, and ligand molecules used in the synthesis. QDs are mainly composed of groups II–VI or III–V elements, such as CdTe, CdS, ZnSe, InP, or InAs, with a size range between 1 and 10 nm, which give rise to quantum confinement effect with narrow emission bands and broad absorbance bands. QDs are also reported to have extended photostability over molecular fluorophores for long-time imaging and prevent photobleaching, high quantum efficacy, the capacity of simultaneous multicolor imaging through single-light source excitation, and ease of modification (Li et al. 2015). Therefore, due to various appealing features of these nanomaterials, the use of QDs in imaging applications has been quickly evolved with comparison to conventional fluorescence dyes (Hildebrandt 2011). For the first time, Murray et al. (1993) reported the synthesis of CdX quantum dots at a high temperature from dimethyl cadmium and trioctylphosphine chalcogenides or hexamethyl disilathiane as base. The synthesized CdX quantum dots were found to be highly hydrophobic and incompatible in the aqueous phase. Thereafter, biocompatible QDs were synthesized from cadmium perchlorate in aqueous phase (Vossmeyer et al. 1994). The problem related to quantum efficiency and size distribution of QDs was further overcome by Peng and Peng (2001) by introducing greener methods for the synthesis of QDs from $Cd(CO_3)_2$, CdO, and $Cd(acetate)_2$. The best-quality quantum dots are synthesized in the organic phase and are capped with highly hydrophobic aliphatic ligands. The ligand exchange reactions and surface modifications are found to be necessary for biological applications of QDs. The most important things that have to be kept in mind during the surface modification of QDs are that the vital properties of QDs should be remained unaffected and uniformly dispersed and the conjugated molecules should also be biocompatible for biological applications. QDs capped with small organic molecules such as thioglycolic acid, dihydrolipoic acid, or mercaptopropionic acid may help in the direct interaction with cells and translocation into the cytosol. QDs conjugated with peptides such as nucleus localization signal or mitochondrial localization signal help in targeted intracellular labeling and imaging of nucleus or mitochondria, respectively. However, nontargeted QDs modified with surface molecules such as polymers, gelatin, carboxylic acids, and polyarginine are also explored for imaging various targeting sites such as blood vessels, lymph nodes, tumors, etc. Moreover, quantum dot–D-lactose conjugates have also been used for targeted labeling and imaging of leukocytes in in vivo applications (Vlasceanu et al. 2017; Martynenko et al. 2017).

15.2.5 Carbon Nanotubes

Carbon nanotubes (CNTs) are one of the most commonly used nanomaterials in the field of healthcare (Kumar et al. 2017). CNTs are constructed as hollow cylindrical tubes consisting of carbon (graphite) with a high aspect ratio and sp^2 hybridization. Depending on the number of graphite layers, CNTs can be classified as single-walled nanotubes (SWNTs), double-walled nanotubes (DWNTs), and multiwalled nanotubes (MWNTs). Carbon nanotubes can be synthesized by various methods including arc discharge, laser ablation, and chemical vapor deposition (CVD). Arc discharge and laser ablation techniques developed earlier generally require high temperature (˃1700˚C) during synthesis, and CVD and their modified CVD methods have replaced these methods as they can be conducted at lower temperatures (˂800 °C). Synthesized CNTs were found to be in the form of aggregate or bundle due to hydrophobic nature, while its uniform suspensions in aqueous buffers have to be used for bioimaging, drug delivery, photothermal therapy, and also in other applications. Dispersion of CNTs in the aqueous phase can be done by controlled sonication of an aqueous suspension of CNTs with amphiphilic molecules or surfactants. Moreover, functionalizations (covalent and noncovalent) are the most effective method for the stable dispersion of CNTs in the organic as well as in the aqueous phase. Fundamental properties responsible for bioimaging are the broad absorption band, outstanding photoacoustic response, NIR photoluminescence, and unique Raman/surface-enhanced Raman scattering effect (Kostarelos et al. 2009). Graphite mode (G-band) of CNT provides the most prevailing fingerprint Raman band for bioimaging. Moreover, its NIR excitation for Raman imaging is helpful in the minimization of autofluorescence of biological specimen and photobleaching of CNTs (Kostarelos et al. 2009). Additionally, photoacoustic imaging property of CNT provides another auspicious technique for bioimaging. CNTs offered excellent photo-to-acoustic conversion efficiency and photothermal–acoustic response, which make these materials one of the most auspicious contrast agents in photoacoustic imaging of tumors (discussed later). Also, conjugated CNTs with radionuclides, fluorescent dyes, other nanoparticles, or inorganic complexes act as contrast agent for various bioimaging techniques such as MRI, CT, PET, SPECT (single-photon emission computed tomography), etc.

15.2.6 Fullerenes

Fullerenes are the zero-dimensional form of graphitic carbon in the form of a hollow sphere, ellipsoid or tube. Spherical fullerenes are also referred to as buckyballs. An important property of C_{60} molecule is its high symmetry, containing 20 hexagons and 12 pentagons. For the first time, it was prepared by the laser vaporization of graphite on a preparative scale; thereafter, Kratschmer–Huffman (1990) introduced its macroscopic-scale synthesis, where a vacuum arc discharge was used for

the synthesis of C_{60} from graphite rods. For enhancement of C_{60} applications, functionalization is very important, and one has to start from its suspension in an organic solvent. Various free-radical reactions like cyclopropanation or cycloaddition reactions can be used for covalent conjugation of C_{60} with molecules.

Partha and Conyers (2009) reported multiple iodine-functionalized C_{60} as a promising X-ray contrast agent, with prolonged retention in the blood and exceptional in vivo biocompatibility when compared with other commercially available X-ray contrast agents such as iopamidol and iohexol. The most interesting properties of C_{60} include absorption light in the UV–vis region, photothermal effect, the ability to accommodate multiple electrons and endohedral metal atoms, long-living triplet state, and singlet oxygen production which added the application of fullerenes in radioimaging, gene/drug delivery, oxidative stress reduction, and cancer therapy.

15.2.7 Graphene

Graphene is an allotrope of carbon in the sp_2-hybridized state with 2D honeycomb lattice, which is the raw material for the synthesis of other types of carbons like fullerene and CNTs. Naturally, graphene is an aromatic structure having many unsaturated carbon–carbon bonds in the plane, which offer free π electrons and reactive sites for surface functionalizations. Graphene has attracted the interest of researchers due to their unique physicochemical properties such as strong mechanical strength, acceptable biocompatibility, ease of production, and ease of modification owing to their versatile surface functionalization and ultrahigh surface area characteristics (Lin et al. 2018). Along with graphene, its other derivatives, such as graphene oxide, reduced graphene oxide, and graphene quantum dots, are also explored in various biomedical fields. For the first time, it was isolated by the exfoliation of graphite using an adhesive tape (Geim and Novoselov 2007). Chemical vapor decomposition on metal substrates or thermal decomposition of carbon-based wafer such as silicon carbide wafer in the presence of ultrahigh vacuum conditions, mechanical exfoliation of highly oriented pyrolytic graphite, and chemical and thermal reduction of graphene oxide are some well-known methods for large-scale production of graphene (Bhuyan et al. 2016). Graphene has poor dispersion in liquids which can be overcome by functionalization. Just like CNTs, graphenes have some fundamental properties like visible and NIR photoluminescence, characteristic Raman bands, and photoacoustic and photothermal responses for bioimaging (Choi et al. 2010).

15.3 Applications of Nanoparticles in Different Bioimaging Modalities

15.3.1 Magnetic Resonance Imaging

Magnetic resonance imaging (MRI) is an imaging technique that is used to study the structure and function of tissues in medical field (Weissleder 2006; Jun et al. 2008; Waters and Wickline 2008). The basis of MRI depends on the behavior, alignment, and interaction of protons which allow for tissue imaging with an enhanced resolution in both space and time in the presence of an applied magnetic field. By applying a strong magnetic field, protons in the tissues are perturbed from the relaxed state and converted into an image. The weakness of the magnetic signal and the low detector sensitivity are usually overcome by introducing contrast agents (CAs) and amplification. Contrast agents are used to alter/shorten the relaxation parameters, i.e., longitudinal (T1) or transverse (T2), which further enhances the contrast between tissues. MRI contrast agents can help clarify images and allow better interpretation. Efficiency of contrast agent is calculated by its reflexivity over a range of concentrations. The radiation dose is being rid off in MRI and thus offers higher spatial resolution when compared to radionuclide-based imaging (Weissleder 2006; Jun et al. 2008; Weissleder and Imhof 2007). Studies of exploration of various nanoparticles to improve contrast in MRI imaging are further explained.

Magnetic nanoparticles are of considerable importance because of their promising use in magnetic, optical, and electronic devices (Thorek et al. 2008; Shi et al. 2008; Asl 2017; Abd-Elsalam et al. 2019). Magnetic nanoparticles have been used in clinics with great success (Sun et al. 2008; Neumaier et al. 2008; Jun et al. 2008) for more than two decades. Highly superparamagnetic iron oxide is generally used as the core material with dextran (biocompatible polymers) as a coating material (Schulze et al. 1995). Advantages of using iron oxide nanoparticles are their biocompatibility, faster detection rate at moderate concentrations, high saturation magnetization, and relatively less toxicity than optical imaging agents. Paramagnetic substances, such as gadolinium (Gd), are positive contrast agents (T1 CA). Due to Gd limitations, certain degree of toxicity, and decreased efficiency at higher magnetic fields, the research focus has shifted to negative CA such as superparamagnetic iron oxide nanoparticles (SPIONs), a T2 CA in MRI (Veiseh et al. 2010). For active targeting, peptides, antibodies, proteins, and small molecules have been conjugated to SPIONs as contrast agent in MRI, due to their tunable properties and their low toxicity compared with gadolinium (Wunderbaldinger et al. 2002a, b). Wunderbaldinger et al. (2002a) have used dextran–SPION to examine the lymph node metastasis in an experimental murine model using contrast-enhanced MRI. In order to visualize tumors better, Montet et al. (2006) have used magnetofluorescent nanoparticle conjugates targeting normal tissues. Bombesin-labeled magnetofluorescent nanoparticles targeting bombesin receptors present on normal acinar cells of the pancreas leads to a decrease in the T2 signal of normal pancreas tissue, thus enhancing the ability to visualize tumors by MRI. Huh and co-workers (2005) produced iron oxide nanoparticles conjugated with Herceptin to detect breast cancers

by MRI. Mn-doped iron oxide nanoparticles have been used for ultrasensitive molecular imaging (Lee et al. 2007). Engineered nanoparticles possessing high magnetism offer improved sensitivity and lower dosing when compared with non-engineered iron oxide contrast agents.

Another type of nanoparticles that have been used in MRI is Fe–Pt nanoparticles. Yang et al. (2010) explored Fe–Pt nanoparticles as possible contrast agents for MRI. Amphiphilic Fe–Pt nanoparticles, which contain both hydrophilic and lipophilic properties, were prepared by high-temperature pyrolysis in a tetraethylene glycol (TEG) medium with oleic acid (OA) as a surfactant. Cell viability studies were carried out on cervical cancer (HeLa) cell lines by taking Fe–Pt nanoparticles to determine the toxic effects. Magnetic properties such as saturation magnetization (Ms) and transverse relaxation time (T2) were also investigated. The MTT assay and transmission electron microscopy (TEM) results depicted that the amphiphilic Fe–Pt nanoparticles were found biocompatible with almost no cytotoxic effect. Magnetic resonance (MR) signal enhancement studies showed clear contrast from the background. It was observed that amphiphilic Fe–Pt nanoparticles could be promisingly used as a *T*2 contrast agent for MRI. Martins et al. (2014) and Carvaldo et al. (2014) reported magnetoliposomes coated with polyethylene glycol (PEG) and loaded with PEGylated SPION as a contrast agent and found PEGylated magnetoliposomes as negative CA for MRI than others. Martínez-González et al. (2016) reported liposomes loaded with hydrophobic iron oxide nanoparticles (SPIONs), i.e., magnetoliposomes as suitable candidates as CAs, especially as a liver CA. Boretti and Castelletto (2016) introduced a nanometric resolution MRI method for noninvasive mapping of functional activity in neuronal networks. Therefore, in the new approach, instead of using SPIONs alone, they can also be encapsulated/embedded in the nanocarrier (liposomes) with a double-function approach in theranostics-like imaging/diagnostics as well as therapy (Carvalho et al. 2017). Recently, chitosan-based SPIONs have been introduced intravenously in orthotopic C6 gliomas in rats which further accumulated in the tumor site, and this retention of nanoparticles resulted in a significant contrast enhancement of the tumor image (Shevtsov et al. 2018).

15.3.2 Computed Tomography

X-ray computed tomography (CT) having optimal cost and broad availability is a commonly used diagnostic imaging tool. X-ray CT helps in visualizing the differences in tissue density and provides image contrast between soft tissues and electron-dense bones. It is often desired to enhance the contrast of the diseased tissue with the use of X-ray contrast agents which increase the contrast between the normal and diseased tissues (Yu and Watson 1999). Commonly used CT contrast enhancers are water-soluble small organic iodinated molecules. The limitations of using these molecules are short imaging times owing to rapid renal clearance and nonspecific vascular permeation (Blaszkiewicz 1994; Yu and Watson 1999; Galperin

et al. 2007; Kim et al. 2007). In order to overcome the problems associated with the use of small organic molecules, nanoparticle contrast agents for CT were developed as early as the 1980s, and after that various nanoparticles have been explored in X-ray CT (Cormode et al. 2014; Mahan and Doiron 2018).

CT was earlier not considered to be a molecular imaging technique like various other techniques, viz., magnetic resonance imaging (MRI), nuclear medicine imaging modalities (SPECT, PET), etc. Cai et al. (2007) used colloidal GNPs as a blood-pool contrast agent for X-ray computed tomography in mice. Furthermore, Popovtzer et al. (2008) reported GNPs conjugated with a targeted moiety for the detection of head and neck cancer with a standard clinical CT. Instead of using spherical gold nanoparticles, they used gold nanorods. It is a prerequisite that in CT imaging, the amount of the gold content per unit volume is important regardless of the particle shape and size. Gold nanorods (synthesized by the method of Nikoobakht and El-Sayed 2003), conjugated with UM-A9 antibodies, have been used to target squamous cell carcinoma (SCC). By this study, it was found that the A9-antibody-coated gold nanorods targeted the SCC cells and showed an increased attenuation coefficient (ΔHU; 168–170) when compared to the nontargeted nanorods, non-cancerous cells (normal fibroblast cells), and other cancerous cells (melanoma) (ΔHU; 28–32). The increased X-ray attenuation in targeted SCC cells compared with normal cells confirms to consider molecular X-ray CT imaging as a molecular imaging technique (Popovtzer et al. 2008). Another study which explored gold nanoparticles (1.9 nm) as an X-ray CT contrast agent was explained by Hainfeld et al. (2006) to diagnose tumors in mice. The injected gold nanoparticles were unable to be present in the blood after 24 h, but instead accumulation in the kidney, tumor, liver, and muscle occurs after just 15 min. The gold nanoparticles are removed from the kidneys by means of renal excretion, and no concentrate was found in the liver or spleen, presumably because of the small size of the nanoparticles. Kattumuri et al. (2007) had made use of gum Arabic stabilized gold nanoparticles as a potential biocompatible X-ray CT contrast agent. Besides GNPs, Fe–Pt nanoparticles are also being used as contrast agents for both computed tomography (CT) and MRI as studied by Chou et al. (2010). The research group also reported that NPs were biocompatible with no cytotoxic effect and no significant hemolysis. Moreover, these NPs were binded to a specific site as well as enhanced the contrast by shortening of T2 relaxation.

Van Schooneveld et al. (2010) synthesized PEGylated gold/silica nanoparticles with paramagnetic and fluorescent lipid coating and applied as trimodal contrast agents to allow for nanoparticle-enhanced imaging of macrophage cells in vitro via MRI, CT, and FI and mice livers in vivo via MRI and CT. Cormode et al. (2010) injected a gold high-density lipoprotein nanoparticle as CA for the characterization of macrophage burden, calcification, and stenosis of atherosclerotic plaques and concluded that the used CA gave multicolor CT images with valuable information about atherosclerotic plaques. Moreover, along with X-ray imaging, chemo-photothermal therapy was also performed by using core–shell-structured docetaxel-loaded PLGA–GNPs, showing significant imaging as well as theranostic approach (Hao et al. 2015). Thereafter, researchers used different types of nanoparticles as CAs for the betterment of CT application along with other imaging modalities

(Pan et al. 2012; Xue et al. 2014; Cole et al. 2015; Chhour et al. 2016; Cheheltani et al. 2016; Si-Mohamed et al. 2017).

15.3.3 Positron Emission Tomography

Positron emission tomography (PET) is an imaging technique which depicts three-dimensional images of biological processes in real time. Three-dimensional images of tracers can be obtained by detecting pairs of gamma rays which are emitted by a tracer (represented by a positron-emitting radionuclide) when conjugated to biologically active molecules. PET becomes one of the most promising techniques for the diagnosis of diseases in a noninvasive manner because of having excellent sensitivity and low background noise. PET is a powerful tool for in vivo imaging of human brain function in neurological disorders such as Parkinson's disease, Huntington's disease, multiple sclerosis, and dementias (Meltzer et al. 2003; Herholz et al. 2007; Politis and Piccini 2012; Assimakopoulos et al. 2014; Niccolini et al. 2015; Kato et al. 2016). Carbon-based nanoparticles have been used for PET imaging. Positron-emitting radionuclides can be conjugated to CNTs or even inserted into CNTs for PET imaging. McDevitt et al. (2007) have produced yttrium-86 (^{86}Y)-CNTs covalently attached to multiple copies of DOTA chelates for the solubilization of functionalized CNTs, and the whole-body PET images depicted that ^{86}Y-CNTs have been cleared from the blood within 3 h and distributed majorly to the kidneys, liver, spleen, and bone in mice. In another study, Ruggiero et al. (2010) constructed SWCNTs covalently attached with radio metal–ion chelates (DOPA) and tumor-targeting antibody and used for rapid imaging. Dynamic and longitudinal PET imaging of LS174T tumor-bearing mice demonstrated rapid blood clearance (<1 h) and specific tumor accumulation of the specific construct. PEGylated GO nanoparticles have been used in PET and have shown minimal toxicity when administrated in mice (Yang et al. 2011). Though CNTs are found to be a potential nanomaterial for diagnostic applications, due to their nonbiodegradability nature, CNTs are still not preferred to be used in PET.

Next comes the use of gold nanoparticles in PET imaging. Xie et al. (2010) reported the use radiolabeled gold nanoshells (NSs) with tumor xenografts to produce in vivo PET images. GNPs coated with the radionuclide, (64)Cu and three types of materials, (64)Cu-NS and the controls ((64)Cu-DOTA and (64)Cu-DOTA-PEG2K) were observed for biodistribution and PET imaging. PET images of the rats showed accumulation of (64)Cu-NSs in the tumors and other organs with significant difference from the controls. In another study by Karmani et al. (2013), ^{89}Zr-labeled antibody-targeted GNPs have proved to be a potential probe for cancer imaging and therapy. The use of metal oxide nanoparticles in the application of PET imaging has also been investigated. Perez–Campana and co-workers (2012) reported the activation of ^{18}O-enriched aluminum oxide (Al_2O_3) NPs by irradiation with protons to yield ^{18}F-labeled NPs. Biodistribution studies were carried out in male rats using ^{18}F-labeled NPs which helps in determining the biodistribution pattern in rodents up to 8 h.

Another research was done by the same group in 2013 to activate aluminum oxide (Al_2O_3) NPs by directly irradiating with protons via the $^{16}O(p,\alpha)^{13}N$ nuclear reaction. For biodistribution studies, the accumulation of ^{13}N-labeled NPs with different sizes in different organs was recorded during the first 68 min after administration and showed the uptake of NPs in the brain was very low regardless of the particle size, and low accumulation of NPs (<2%) was observed in the lung for smaller NPs as compared to NPs with larger sizes. Some reports are also available for the use of 18F-fluorodeoxyglucose–PET scans for imaging pancreatic cancer and gastric cancer and also for estimation of perimenopause and emergence of an Alzheimer's in the brain (Ma et al. 2013; Crippa et al. 2014; Grimmer et al. 2016; Mosconi et al. 2017). Radiolabeled iron oxide, another class of NPs, is applied for PET imaging. The iron oxide NPs (IONPs) are differentiated into various classes based on their sizes, viz., standard superparamagnetic iron oxide (SPIO) at 60–150 nm, ultrasmall superparamagnetic iron oxide (USPIO) of approximately 5–40 nm, and monocrystalline iron oxide nanocompounds (MION), a subset of USPIO, ranging from 10 to 30 nm (Xing et al. 2014). Among all, SPIONPs have been selected due to exclusive properties of biocompatibility and intrinsic ability to facilitate surface modification, making them attractive as multifunctional imaging agents. Recent applications of radiolabeled iron oxide nanoparticles for PET imaging and multimodality imaging have been summarized in different comprehensive reviews (Bouziotis et al. 2012; Thomas et al. 2013). Combining PET imaging with the other imaging modalities like X-ray CT or MRI provides the synergistic combination of information (Wang et al. 2014; Riola-Parada et al. 2016; Szyszko and Cook 2017).

15.3.4 Ultrasound Imaging

Ultrasound imaging (USI) is a clinical diagnostic technique that is frequently used because of its distinguished properties, namely, its real-time monitoring capability, low cost, high safety, convenience, and portability (Liu et al. 2011). Ultrasound contrast agents (UCAs) in the form of nanoparticles have been developed for improvement in visualization in US imaging. Mattrey et al. (1982) studied the use of PFOB (perfluoroctylbromide) NPs in US imaging. PFOB NPs have considerably increased the echogenicity of the liver as compared to that of the kidney after 48 h of intravenous infusion and produced an echogenic rim around VX2 carcinoma, which helps in tumor diagnosis. By this study, the authors have considered PFOB NPs to be a promising US contrast material. Lanza et al. (1996) found liquid PFC-filled NPs to be used as new UCAs because of having long circulation half-life and high stability. These NPs present a low intensity of US reflection and require higher concentrations or more binding events, which form the physical basis of the ability of PFOB NPs to serve as UCAs and to produce comparatively high backscatter signal (Marsh et al. 2002; Wickline et al. 2002). Horie et al. (2011) studied the antitumor effects of tumor necrosis factor (TNF-α) by transfection of TNF-α plasmid DNA into solid mouse tumors using the nanobubbles (NBs) and ultrasound gene

delivery system. The contrast of the image was enhanced using Sonazoid and a high-frequency US imaging system (40 MHz) to check the difference in tumor size before and after the treatment and found significant reduction in the tumor size. Finally, they concluded the effectiveness of NBs and US for TNF-α gene delivery into tumor cells. Another investigation was done by using halloysite clay nanotubes (HNTs) as promising contrast agents for ultrasound-targeted imaging at a conventional diagnostic frequency of 10 MHz (Conversano et al. 2016). HNTs in the radiofrequency backscatter signals have been used to generate tailored color maps. These were then allowed to superimpose on conventional B-mode echographic images for automated HNT detection having sensitivity up to 60% and specificity above 95% by using HNT concentration of 1.5 mg/mL. HNTs have been found to result in significant diagnostic improvements, enabling nonionizing identification of pathological tissues at cellular level.

15.3.5 Fluorescence Imaging

Fluorescence imaging (FI) has emerged as an evolutionary field that has many significant advancements. This technique has the accumulative availability of fluorescent proteins, dyes, and probes, as well as the development of optical imaging technologies (Ntziachristos 2006). Fluorescence imaging has several advantages like good sensitivity, noninvasive nature, read availability, and comparatively low cost. Because it is an optical technique, it has limitations in terms of tissue penetration depth.

A large number of studies have proved the potential of QDs in the application of fluorescence imaging. Akerman et al. (2002) have used CdSe/Zns QDs coated with PEG for targeting peptides in the lungs of mice. Multifunctional nanoparticle probes based on QDs were formed for in vivo imaging of human prostate cancer in mice, as described by Gao et al. (2004). This new type of coated QDs is based on the encapsulation of PEGylated QDs using an ABC triblock copolymer as a secondary coating layer, further functionalized with a tumor-targeting antibody to prostate-specific membrane antigen. Cai et al. (2006) have conjugated QDs with peptides for targeted in vivo imaging of tumors. As observed from NIR fluorescence images, they showed that QDs labeled with arginine–glycine–aspartic acid (RGD) peptide had selectively target the αvβ3-positive tumor vasculature in a murine xenograft model. Though significant accumulation in the liver, bone marrow and lymph nodes were found, after 6 h of injection of QDs, then also high tumor contrast was there. Distribution of four QDs with different surface coatings was studied by Ballou et al. (2004), and it was observed that the QDs were fluorescent for at least 4 months in vivo. Tada et al. (2007) has chased single QDs coated with monoclonal anti-HER2 antibody using a high-speed confocal microscope in the tumors of living mice in the dorsal skinfold chamber. QD-based contrast agent for brain imaging has been developed by Gao et al. (2008). Surface modification of QDs using poly(ethylene glycol)–poly(lactic acid) was carried out which was then functionalized with wheat germ agglutinin. The

agent was delivered to the brain by means of intranasal administration, and accumulation in the brain remained for >4 h and was cleared after 8 h of administration. Deliberate addition of different components like gadolinium and manganese in QDs leads to the formation of multimodal imaging agents (Yong 2009).

Jin et al. (2008) have produced hybrid QDs with the careful incorporation of Gd^{3+} in QDs to achieve dual-mode (fluorescence/magnetic resonance) imaging. In the same way, Yong (2009) have produced manganese-doped QDs as multimodal targeted probes for pancreatic cancer imaging. To determine the location of anti-claudin, anti-mesothelin, or anti-PSCA-coated QDs to pancreatic cancer cells, confocal spectroscopy was used. The use of Fe–Pt nanoparticles for fluorescence imaging and MRI was studied by Lai et al. (2012). Fe–Pt nanoparticles were formed by a method using high-temperature chemical reduction. The nanoparticles were then coated with silica using a microemulsion method to improve biocompatibility and bioconjugation. This made it easier to incorporate fluorescent dye fluorescein isothiocyanate (FITC) into the silica shell. The cytotoxicity of Fe–Pt and Fe–Pt/SiO_2/FITC nanoparticles was determined by MTT assay using a human cervical cancer cell line (HeLa) and was found nontoxic. Confocal laser microscopy was used to examine the intracellular localization of Fe–Pt/SiO_2/FITC nanoparticles in HeLa cells after staining with a red fluorescent dye, and the fluorescence was observed after 12 h of incubation. These results showed the potential use of Fe–Pt/SiO_2/FITC nanoparticles for dual fluorescence and MR imaging. In another study carried out by Zhang et al. (2016), fluorescent SNPs were developed for application in both in vitro and in vivo fluorescence bioimaging. They are easy to handle, biocompatible in nature, less toxic, and highly hydrophilic and exhibit good optical transparency. Due to these properties, SNPs are considered to be suitable substrates for the fabrication of fluorescent probes and thus can be used in the imaging of living cells.

15.3.6 Photoacoustic Imaging (PAI)

PAI is a new method that has taken the advantages of the same optical properties as that of fluorescence imaging. Tissues are firstly irradiated with visible or near-infrared light, resulting in adiabatic expansion, and thus pressure waves are produced, which in turn are measured and used to construct an image. In cases where depth of penetration is found lower and there is a lack of natural contrast between tissues, contrast agents in the form of various nanoparticles are used (Wu et al. 2014). Zerda et al. (2008) first took photoacoustic images in a tumor mouse model, using SWNTs as the contrast agent. Yang et al. (2010) studied four different types of nanoparticles that can be used as photoacoustic contrast agents in photoacoustic imaging. They focused mainly on gold nanoshells, gold nanorods, gold nanocages, and indocyanine green (ICG)-doped nanoparticles. Their studies found that among the four kinds of nanoparticles employed in PAI so far, nanorods were appropriate optical absorbers. Au nanocages also have similar optical absorption as Au nanorods. In addition, nanocages were found capable of encapsulating drugs and ICG-based

nanoparticles, which depends on the fact that ICG is the FDA-approved dye for routine clinical use. Kim et al. (2009) reported the growth of GNPs on the surface of CNTs and utilized this conjugate as a photoacoustic contrast agent for in vivo imaging and for killing cancer cells via a photothermal effect. Chanda et al. (2011) explored the use of cinnamon phytochemicals as an AuNP capping agent to increase uptake of particles to cancer cells. The results showed linear photoacoustic response from untreated cells, while treated cells showed a time-variant signal, which indicates the particle uptake and particle contrast ability. In another study, Jing et al. (2014) used the fluorescent dye Prussian blue as a coating to enhance the photoacoustic signal. Testing of particles was carried out in agar gels as well as mice using a 765 nm laser. In the absence of tissue, high resolution was found, while an increasing loss of clarity was evident up to ~4.3 cm. Cheheltani et al. (2016) has encapsulated AuNP into polydi (carboxylatophenoxy) phosphazene (PCPP) nanospheres and found that the formulated particles exhibited high CT contrast, while the absorbable wavelengths can be adjusted changing the size or amount of AuNP. Photoacoustic imaging is an emerging field, and researchers use this as a guided technology for photodynamic therapy and photothermal therapy using different PA agents conjugated with different types of nanomaterials (Wang et al. 2016; Xie et al. 2016; Gao et al. 2017; Wu et al. 2017). Photoacoustic imaging is still a new modality imaging technique, further work on the use of different nanoparticles is being carried out to completely understand the parameters of photoacoustic imaging.

15.4 Conclusion

Nanomaterial drastically inflates the proficiencies of conventional methods of imaging owing to their high surface area, controllable size, and ease in surface functionalization. Different types of molecules including small organic dyes, radioisotopes, metal ions, inorganic nanoparticles, and even the source of microbubbles can be easily conjugated to allow an enhanced imaging performance with high stability of imaging agents before delivery to the target cells or organs. In the past few years, lots of studies have been done on the use of nanomaterial for bioimaging applications. However, most of studies are in their infancy stage within finite prospects, and only few have got clinical successes. For in vivo applications, the issues like biocompatibility, systemic toxicity, and unwanted accumulation in the body have to be considered. Imaging efficiencies are also an important factor for bioimaging, which can be improved by the conjugation of targeting ligands such as antibody and peptides, to secure high colloidal stability in the bloodstream. Thus, more efforts are still needed to be done in the near future for the promotion of nanomaterial advances in bioimaging applications.

References

Abd-Elsalam K, Mohamed AA, Prasad R (2019) Magnetic nanostructures: environmental and agricultural applications. Springer International Publishing (ISBN 978-3-030-16438-6) https://www.springer.com/gp/book/9783030164386

Akerman ME, Chan WCW, Laakkonen P, Bhatia SN, Ruoslahti E (2002) Nanocrystal targeting in vivo. Proc Natl Acad Sci USA 99(20):12617–12621

Asl HM (2017) Applications of nanoparticles in magnetic resonance imaging: a comprehensive review. Asian J Pharm 11:S7–S13

Assimakopoulos A, Polyzoidis K, Sioka C (2014) Positron emission tomography imaging in gliomas. Neuroimmunol Neuroinflammation 1(3):107

Ballou B, Lagerholm BC, Ernst LA, Bruchez MP, Waggoner AS (2004) Noninvasive imaging of quantum dots in mice. Bioconjug Chem 15(1):79–86

Bhuyan MSA, Uddin MN, Islam MM, Bipasha FA, Hossain SS (2016) Synthesis of graphene. Int Nano Lett 6(2):65–83

Biju V (2014) Chemical modifications and bioconjugate reactions of nanomaterials for sensing, imaging, drug delivery and therapy. Chem Soc Rev 43(3):744–764

Blaszkiewicz P (1994) Synthesis of water-soluble ionic and nonionic iodinated X-Ray contrast-media. Invest Radiol 29:S51–S53

Boretti A, Castelletto S (2016) Nanometric resolution magnetic resonance imaging methods for mapping functional activity in neuronal networks. Methods X 3:297–306

Bouziotis P, Psimadas D, Tsotakos T, Stamopoulos D, Tsoukalas C (2012) Radiolabeled iron oxide nanoparticles as dual-modality SPECT/MRI and PET/MRI agents. Curr Top Med Chem 12:2694–2702

Brust M, Walker M, Bethell D, Schiffrin DJ, Whyman R (1994) Synthesis of thiol-derivatised gold nanoparticles in a two-phase Liquid–Liquid system. J Chem Soc Chem Commun 7:801–802

Cai WB, Shin DW, Chen K, Gheysens O, Cao Q, Wang SX, Gambhir SS, Chen X (2006) Peptide-labeled near-infrared quantum dots for imaging tumor vasculature in living subjects. Nano Lett 6(4):669–676

Cai QY, Kim SH, Choi KS, Kim SY, Byun SJ, Kim KW, Park SH, Juhng SK, Yoon KH (2007) Colloidal gold nanoparticles as a blood-pool contrast agent for X-ray computed tomography in mice. Invest Radiol 42(12):797–806

Carvalho A, Martins MBF, Corvo ML, Feio G (2014) Enhanced contrast efficiency in MRI by PEGylated magnetoliposomes loaded with PEGylated SPION: effect of SPION coating and micro-environment. Mater Sci Eng C 43:521–526

Carvalho A, Gonçalves MC, Corvo ML, Martins MBF (2017) Development of new contrast agents for imaging function and metabolism by magnetic resonance imaging. Magn Reson Insights. https://doi.org/10.1177/1178623X17722134

Chanda N, Shukla R, Zambre A, Mekapothula S, Kulkarni RR, Katti K, Bhattacharyya K, Fent GM, Casteel SW, Boote EJ, Viator JA (2011) An effective strategy for the synthesis of biocompatible gold nanoparticles using cinnamon phytochemicals for phantom CT imaging and photoacoustic detection of cancerous cells. Pharm Res 28(2):279–291

Cheheltani R, Ezzibdeh RM, Chhour P, Pulaparthi K, Kim J, Jurcova M, Hsu JC, Blundell C, Litt HI, Ferrari VA, Allcock R (2016) Tunable, biodegradable gold nanoparticles as contrast agents for computed tomography and photoacoustic imaging. Biomaterials 102:87–97

Cherukula K, ManickavasagamLekshmi K, Uthaman S, Cho K, Cho CS, Park IK (2016) Multifunctionalinorganic nanoparticles: recent progress in thermal therapy and imaging. Nanomaterials 6(4):76

Chhour P, Naha PC, O'Neill SM, Litt HI, Reilly MP, Ferrari VA, Cormode DP (2016) Labeling monocytes with gold nanoparticles to track their recruitment in atherosclerosis with computed tomography. Biomaterials 87:93–103

Choi W, Lahiri I, Seelaboyina R, Kang YS (2010) Synthesis of graphene and its applications: a review. Crit Rev Solid State Mater Sci 35(1):52–71

Chou SW, Shau YH, Wu PC, Yang YS, Shieh DB, Chen CC (2010) *In vitro* and *in vivo* studies of FePt nanoparticles for dual modal CT/MRI molecular imaging. J Am Chem Soc 132(38):13270–13278

Cole LE, Ross RD, Tilley JM, Vargo-Gogola T, Roeder RK (2015) Gold nanoparticles as contrast agents in x-ray imaging and computed tomography. Nanomedicine 10(2):321–341

Contado C, Ravani L, Passarella M (2013) Size characterization by sedimentation field flow fractionation of silica particles used as food additives. Anal Chim Acta 788:183–192

Conversano F, Pisani P, Casciaro E, di Paola M, Leporatti S, Franchini R, Quarta A, Gigli G, Casciaro S (2016) Automatic echographic detection of halloysite clay nanotubes in a low concentration range. Nanomaterials 6:66

Cormode DP, Roessl E, Thran A, Skajaa T, Gordon RE, Schlomka JP, Fuster V, Fisher EA, Mulder WJ, Proksa R, Fayad ZA (2010) Atherosclerotic plaque composition: analysis with multicolor CT and targeted gold nanoparticles. Radiology 256(3):774–782

Cormode DP, Naha PC, Fayad ZA (2014) Nanoparticle contrast agents for computed tomography: a focus on micelles. Contrast Media Mol Imaging 9(1):37–52

Crippa S, Salgarello M, Laiti S, Partelli S, Castelli P, Spinelli AE, Tamburrino D, Zamboni G, Falconi M (2014) The role of 18fluoro-deoxyglucose positron emission tomography/computed tomography in resectable pancreatic cancer. Dig Liver Dis 46(8):744–749

Dreaden EC, Alkilany AM, Huang X, Murphy CJ, El-Sayed MA (2012) The golden age: gold nanoparticles for biomedicine. Chem Soc Rev 41(7):2740–2779

Galperin A, Margel D, Baniel J, Dank G, Biton H, Margel S (2007) Radiopaque iodinated polymeric nanoparticles for X-ray imaging applications. Biomaterials 28(30):4461–4468

Gao XH, Cui YY, Levenson RM, Chung LW, Nie S (2004) *In vivo* cancer targeting and imaging with semiconductor quantum dots. Nat Biotechnol 22(8):969

Gao XL, Chen J, Chen JY, Wu B, Chen H, Jiang X (2008) Quantum dots bearing lectin-functionalized nanoparticles as a platform for in vivo brain imaging. Bioconjug Chem 19(11):2189–2195

Gao S, Wang G, Qin Z, Wang X, Zhao G, Ma Q, Zhu L (2017) Oxygen-generating hybrid nanoparticles to enhance fluorescent/photoacoustic/ultrasound imaging guided tumor photodynamic therapy. Biomaterials 112:324–335

Geim AK, Novoselov KS (2007) The rise of graphene. Nat Mater 6:183–191

Grimmer T, Wutz C, Alexopoulos P, Drzezga A, Förster S, Förstl H, Goldhardt O, Ortner M, Sorg C, Kurz A (2016) Visual versus fully automated analyses of 18F-FDG and amyloid PET for prediction of dementia due to Alzheimer disease in mild cognitive impairment. J Nucl Med 57(2):204–207

Hainfeld JF, Slatkin DN, Smilowitz HM (2004) The use of gold nanoparticles to enhance radiotherapy in mice. Phys Med Biol 49(18):N309–N315

Hainfeld JF, Slatkin DN, Focella TM, Smilowitz HM (2006) Gold nanoparticles: a new X-ray contrast agent. Br J Radiol 79(939):248–253

Hao Y, Zhang B, Zheng C, Ji R, Ren X, Guo F, Sun S, Shi J, Zhang H, Zhang Z, Wang L (2015) The tumor-targeting core–shell structured DTX-loaded PLGA@ Au nanoparticles for chemo-photothermal therapy and X-ray imaging. J Control Release 220:545–555

Herholz K, Carter SF, Jones M (2007) Positron emission tomography imaging in dementia. Br J Radiol 80(2):S160–S167

Hildebrandt N (2011) Biofunctional quantum dots: controlled conjugation for multiplexed biosensors. ACS Nano 5(7):5286–5290

Horie S, Watanabe Y, Ono M, Mori S, Kodama T (2011) Evaluation of antitumor effects following tumor necrosis factor-α gene delivery using nanobubbles and ultrasound. Cancer Sci 102(11):2082–2089

Huh YM, Jun YW, Song HT, Kim S, Choi JS, Lee JH, Yoon S, Kim KS, Shin JS, Suh JS, Cheon J (2005) *In vivo* magnetic resonance detection of cancer by using multifunctional magnetic nanocrystals. J Am Chem Soc 127(35):12387–12391

Jin T, Yoshioka Y, Fujii F, Komai Y, Seki J, Seiyama A (2008) Gd3+−functionalized near-infrared quantum dots for in vivo dual modal (fluorescence/magnetic resonance) imaging. Chem Commun 44:5764–5766

Jing L, Liang X, Deng Z, Feng S, Li X, Huang M, Li C, Dai Z (2014) Prussian blue coated gold nanoparticles for simultaneous photoacoustic/CT bimodal imaging and photothermal ablation of cancer. Biomaterials 35(22):5814–5821

Jun YW, Lee JH, Cheon J (2008) Chemical design of nanoparticle probes for high-performance magneticresonance imaging. Angew Chem Int Ed 47(28):5122–5135

Karmani L, Labar D, Valembois V, Bouchat V, Nagaswaran PG, Bol A, Gillart J, Levêque P, Bouzin C, Bonifazi D, Michiels C (2013) Antibody-functionalized nanoparticles for imaging cancer: influence of conjugation to gold nanoparticles on the biodistribution of 89Zr-labeled cetuximab in mice. Contrast Media Mol Imaging 8(5):402–408

Kato T, Inui Y, Nakamura A, Ito K (2016) Brain fluorodeoxyglucose (FDG) PET in dementia. Ageing Res Rev 30:73–84

Kattumuri V, Katti K, Bhaskaran S, Boote EJ, Casteel SW, Fent GM, Robertson DJ, Chandrasekhar M, Kannan R, Katti KV (2007) Gum arabic as a phytochemical construct for the stabilization of gold nanoparticles: *in vivo* pharmacokinetics and X-ray-contrast-imaging studies. Small 3(2):333–341

Kim D, Park S, Lee JH, Jeong YY, Jon S (2007) Antibiofouling polymer-coated gold nanoparticles as a contrast agent for in vivo X-ray computed tomography imaging. J Am Chem Soc 129:7661–7665

Kim JW, Galanzha EI, Shashkov EV, Moon HM, Zharov VP (2009) Golden carbon nanotubes as multimodal photoacoustic and photothermal high-contrast molecular agents. Nat Nanotechnol 4:688–694

Kostarelos K, Bianco A, Prato M (2009) Promises, facts and challenges for carbon nanotubes in imaging and therapeutics. Nat Nanotechnol 4(10):627–633

Krätschmer W, Lamb LD, Fostiropoulos K, Huffman DR (1990) Solid C60: a new form of carbon. Nature 347(6291):354

Kumar S, Rani R, Dilbaghi N, Tankeshwar K, Kim KH (2017) Carbon nanotubes: a novel material for multifaceted applications in human healthcare. Chem Soc Rev 46(1):158–196

Lai SM, Tsai TY, Hsu CY, Tsai JL, Liao MY, Lai PS (2012) Bifunctional silica-coated superparamagnetic FePt nanoparticles for fluorescence/MR dual imaging. J Nanomater 2012:5

Lanza GM, Wallace KD, Scott MJ, Cacheris WP, Abendschein DR, Christy DH, Sharkey AM, Miller JG, Gaffney PJ, Wickline SA (1996) A novel site-targeted ultrasonic contrast agent with broad biomedical application. Circulation 94(12):3334–3340

Laurent S, Forge D, Port M, Roch A, Robic C, Vander Elst L, Muller RN (2008) Magnetic iron oxide nanoparticles: synthesis, stabilization, vectorization, physicochemical characterizations, and biological applications. Chem Rev 108(6):2064–2110

Lee JH, Huh YM, Jun YW, Seo JW, Jang JT, Song HT, Kim S, Cho EJ, Yoon HG, Suh JS, Cheon J (2007) Artificially engineered magnetic nanoparticles for ultra-sensitive molecular imaging. Nat Med 13(1):95

Lee N, Cho HR, Oh MH, Lee SH, Kim K, Kim BH, Shin K, Ahn TY, Choi JW, Kim YW, Choi SH (2012) Multifunctional Fe_3O_4/TaO x Core/Shell nanoparticles for simultaneous magnetic resonance imaging and X-ray computed tomography. J Am Chem Soc 134(25):10309–10312

Li J, Cheng F, Huang H, Li L, Zhu JJ (2015) Nanomaterial-based activatable imaging probes: from design to biological applications. Chem Soc Rev 44(21):7855–7880

Liang S, Zhou Q, Wang M, Zhu Y, Wu Q, Yang X (2015) Water-soluble l-cysteine-coated FePt nanoparticles as dual MRI/CT imaging contrast agent for glioma. Int J Nanomed 10:2325

Lin J, Huang Y, Huang P (2018) Graphene-based nanomaterials in bioimaging. In: Biomedical applications of functionalized nanomaterials. Elsevier, pp 247–287

Liu Z, Lammers T, Ehling J, Fokong S, Bornemann J, Kiessling F, Gätjens J (2011) Iron oxide nanoparticle-containing microbubble composites as contrast agents for MR and ultrasound dual-modality imaging. Biomaterials 32(26):6155–6163

Ma DW, Kim JH, Jeon TJ, Lee YC, Yun M, Youn YH, Park H, Lee SI (2013) F-fluorodeoxyglucose positron emission tomography-computed tomography for the evaluation of bone metastasis in patients with gastric cancer. Dig Liver Dis 45(9):769–775

Mahan MM, Doiron AL (2018) Gold nanoparticles as X-ray, CT, and multimodal imaging contrast agents: formulation, targeting, and methodology. J Nanomater. https://doi.org/10.1155/2018/5837276

Marsh JN, Hall CS, Scott MJ, Fuhrhop RW, Gaffney PJ, Wickline SA, Lanza GM (2002) Improvements in the ultrasonic contrast of targeted perfluorocarbon nanoparticles using an acoustic transmission line model. IEEE Trans Ultrason Ferroelectr Freq Control 49(1):29–38

Martínez-González R, Estelrich J, Busquets MA (2016) Liposomes loaded with hydrophobic iron oxide nanoparticles: suitable T2 contrast agents for MRI. Int J Mol Sci 17(8):1209

Martins MBA, Corvo ML, Marcelino P, Marinho HS, Feio G, Carvalho A (2014) New long circulating magnetoliposomes as contrast agents for detection of ischemia-reperfusion injuries by MRI. Nanomed Nanotechnol 10(1):207–214

Martynenko IV, Litvin AP, Purcell-Milton F, Baranov AV, Fedorov AV, Gun'ko YK (2017) Application of semiconductor quantum dots in bioimaging and biosensing. J Mater Chem B 5(33):6701–6727

Mattrey RF, Scheible FW, Gosink BB, Leopold GR, Long DM, Higgins CB (1982) Perfluoroctylbromide: aliver/spleen-specific and tumor-imaging ultrasound contrast material. Radiology 145(3):759–762

McDevitt MR, Chattopadhyay D, Jaggi JS, Finn RD, Zanzonico PB, Villa C, Rey D, Mendenhall J, Batt CA, Njardarson JT, Scheinberg DA (2007) PET imaging of soluble yttrium-86-labeled carbon nanotubes in mice. PLoS One 2(9):e907

Meltzer CC, Becker JT, Price JC, Moses-Kolko E (2003) Positron emission tomography imaging of the aging brain. Neuroimaging Clin 13(4):759–767

Montet X, Weissleder R, Josephson L (2006) Imaging pancreatic cancer with a peptide-nanoparticle conjugate targeted to normal pancreas. Bioconjug Chem 17(4):905–911

Mosconi L, Berti V, Guyara-Quinn C, McHugh P, Petrongolo G, Osorio RS, Connaughty C, Pupi A, Vallabhajosula S, Isaacson RS, de Leon MJ (2017) Perimenopause and emergence of an Alzheimer's bioenergetic phenotype in brain and periphery. PLoS One 12(10):e0185926

Murphy CJ, Gole AM, Hunyadi SE, Stone JW, Sisco PN, Alkilany A, Kinard BE, Hankins P (2008) Chemical sensing and imaging with metallic nanorods. Chem Commun 5:544–557

Murray C, Norris DJ, Bawendi MG (1993) Synthesis and characterization of nearly monodisperse CdE (E= sulfur, selenium, tellurium) semiconductor nanocrystallites. J Am Chem Soc 115(19):8706–8715

Neumaier CE, Baio G, Ferrini S, Corte G, Daga A (2008) MR and iron magnetic nanoparticles. Imaging opportunities in preclinical and translational research. Tumori J 94(2):226–233

Niccolini F, Su P, Politis M (2015) PET in multiple sclerosis. Clin Nucl Med 40(1):e46–e52

Nikoobakht B, El-Sayed MA (2003) Preparation and growth mechanism of gold nanorods (NRs) using seed-mediated growth method. Chem Mater 15(10):1957–1962

Ntziachristos V (2006) Fluorescence molecular imaging. Annu Rev Biomed Eng 8:1–33

Ow H, Larson DR, Srivastava M, Baird BA, Webb WW, Wiesner U (2005) Bright and stable core−shell fluorescent silica nanoparticles. Nano Lett 5(1):113–117

Pan D, Schirra CO, Senpan A, Schmieder AH, Stacy AJ, Roessl E, Thran A, Wickline SA, Proska R, Lanza GM (2012) An early investigation of ytterbium nanocolloids for selective and quantitative "multicolor" spectral CT imaging. ACS nano 6(4):3364–3370

Partha R, Conyers JL (2009) Biomedical applications of functionalized fullerene-based nanomaterials. Int J Nanomed 4:261–275

Peng ZA, Peng X (2001) Formation of high-quality CdTe, CdSe, and CdS nanocrystals using CdO as precursor. J Am Chem Soc 123(1):183–184

Pérez-Campaña C, Gómez-Vallejo V, Martin A, San Sebastián E, Moya SE, Reese T, Ziolo RF, Llop J (2012) Tracing nanoparticles in vivo: a new general synthesis of positron emitting metal oxide nanoparticles by proton beam activation. Analyst 137:4902–4906

Politis M, Piccini P (2012) Positron emission tomography imaging in neurological disorders. J Neurol 259(9):1769–1780

Popovtzer R, Agrawal A, Kotov NA, Popovtzer A, Balter J, Carey TE, Kopelman R (2008) Targeted gold nanoparticles enable molecular CT imaging of cancer. Nano Lett 8(12):4593–4596

Reddy LH, Arias JL, Nicolas J, Couvreur P (2012) Magnetic nanoparticles: design and characterization, toxicity and biocompatibility, pharmaceutical and biomedical applications. Chem Rev 112(11):5818–5878

Riola-Parada C, García-Cañamaque L, Pérez-Dueñas V, Garcerant-Tafur M, Carreras-Delgado JL (2016) Simultaneous PET/MRI vs. PET/CT in oncology. A systematic review. Revista Española de Medicina Nucleare Imagen Molecular (English Edition) 35(5):306–312

Ruggiero A, Villa CH, Holland JP, Sprinkle SR, May C, Lewis JS, Scheinberg DA, McDevitt MR (2010) Imaging and treating tumor vasculature with targeted radiolabeled carbon nanotubes. Int J Nanomedicine 5:783

Saha K, Agasti SS, Kim C, Li X, Rotello VM (2012) Gold nanoparticles in chemical and biological sensing. Chem Rev 112(5):2739–2779

Schulze E, Ferrucci JT, Poss K, Lapointe L, Bogdanova A, Weissleder R (1995) Cellular uptake and trafficking of a prototypical magnetic iron-oxide label *in-vitro*. Invest Radiol 30(10):604–610

Shevtsov M, Nikolaev B, Marchenko Y, Yakovleva L, Skvortsov N, Mazur A, Tolstoy P, Ryzhov V, Multhoff G (2018) Targeting experimental orthotopic glioblastoma with chitosan-based superparamagnetic iron oxide nanoparticles (CS-DX-SPIONs). Int J Nanomed 13:1471

Shi XY, Wang SH, Swanson SD, Ge S, Cao Z, Van Antwerp ME, Landmark KJ, Baker Jr (2008) Dendrimer-functionalized shell-crosslinked iron oxide nanoparticles for *in-vivo* magnetic resonance imaging of tumors. Adv Mater 20(9):1671–1678

Shi P, Qu K, Wang J, Li M, Ren J, Qu X (2012) pH-responsive NIR enhanced drug release from gold nanocages possesses high potency against cancer cells. Chem Commun 48(61):7640–7642

Si-Mohamed S, Cormode DP, Bar-Ness D, Sigovan M, Naha PC, Langlois JB, Chalabreysse L, Coulon P, Blevis I, Roessl E, Erhard K (2017) Evaluation of spectral photon counting computed tomography K-edge imaging for determination of gold nanoparticle biodistribution in vivo. Nanoscale 9(46):18246–18257

Sun C, Lee JSH, Zhang MQ (2008) Magnetic nanoparticles in MR imaging and drug delivery. Adv Drug Deliv Rev 60(11):1252–1265

Szyszko TA, Cook GJR (2017) PET/CT and PET/MRI in head and neck malignancy. Clin Radiol. https://doi.org/10.1016/j.crad.2017.09.001

Tada H, Higuchi H, Wanatabe TM, Ohuchi N (2007) In vivo real-time tracking of single quantum dots conjugated with monoclonal anti-HER2 antibody in tumors of mice. Cancer Res 67(3):1138–1144

Templeton AC, Wuelfing WP, Murray RW (2000) Monolayer-protected cluster molecules. Acc Chem Res 33(1):27–36

Thomas R, Park IK, Jeong YY (2013) Magnetic iron oxide nanoparticles for multimodal imaging and therapy of cancer. Int J Mol Sci 14:15910–15930

Thorek DL, Czupryna J, Chen AK, Tsourkas A (2008) Molecular imaging of cancer with superparamagnetic iron-oxide nanoparticles. In: Cancer imaging. Academic press, pp 85–95.

Trewyn BG, Slowing II, Giri S, Chen HT, Lin VSY (2007) Synthesis and functionalization of a mesoporous silica nanoparticle based on the sol-gel process and applications in controlled release. Acc Chem Res 40(9):846–853

van Schooneveld MM, Cormode DP, Koole R, van Wijngaarden JT, Calcagno C, Skajaa T, Hilhorst J, Hart DCT, Fayad ZA, Mulder WJ, Meijerink A (2010) A fluorescent, paramagnetic and PEGylated gold/silica nanoparticle for MRI, CT and fluorescence imaging. Contrast Media Mol Imaging 5(4):231–236

Veiseh O, Gunn JW, Zhang M (2010) Design and fabrication of magnetic nanoparticles for targeted drug delivery and imaging. Adv Drug Deliv Rev 62(3):284–304

Vlasceanu G, Grumezescu AM, Gheorghe I, Chifiriuc MC, Holban AM (2017) Quantum dots for bioimaging and therapeutic applications. In: Nanostructures for novel therapy. Elsevier, pp 497–515

Vossmeyer T, Katsikas L, Giersig M, Popovic IG, Diesner K, Chemseddine A, Eychmüller A, Weller H (1994) CdS nanoclusters: synthesis, characterization, size dependent oscillator strength, temperature shift of the excitonic transition energy, and reversible absorbance shift. J Phys Chem 98(31):7665–7673

Wang SC, Xie Q, Lv WF (2014) Positron emission tomography/computed tomography imaging and rheumatoid arthritis. Int J Rheum Dis 17(3):248–255

Wang G, Zhang F, Tian R, Zhang L, Fu G, Yang L, Zhu L (2016) Nanotubes-Embedded Indocyanine Green-Hyaluronic Acid Nanoparticles for Photoacoustic-Imaging-Guided Phototherapy. ACS Appl Mater Interfaces 8(8):5608–5617

Waters EA, Wickline SA (2008) Contrast agents for MRI. Basic Res Cardiol 103(2):114–121

Weissleder R (2006) Molecular imaging in cancer. Science 312(5777):1168–1171

Weissleder R, Imhof H (2007) Molecular imaging – a new focal point of radiology. Der Radiologe 47(1):6–7

Wickline SA, Hughes M, Ngo FC, Hall CS, Marsh JN, Brown PA, Allen JS, McLean MD, Scott MJ, Fuhrhop RW, Lanza GM (2002) Blood contrast enhancement with a novel, non-gaseous nanoparticle contrast agent. Acad Radiol 9(suppl 2):S290–S293

Wu SH, Mou CY, Lin HP (2013) Synthesis of mesoporous silica nanoparticles. Chem Soc Rev 42(9):3862–3875

Wu D, Huang L, Jiang MS, Jiang H (2014) Contrast agents for photoacoustic and thermoacoustic imaging: a review. Int J Mol Sci 15(12):23616–23639

Wu C, Li D, Wang L, Guan X, Tian Y, Yang H, Li S, Liu Y (2017) Single wavelength light-mediated, synergistic bimodal cancer photoablation and amplified photothermal performance by graphene/gold nanostar/photosensitizer theranostics. Acta Biomater 53:631–642

Wunderbaldinger P, Josephson L, Bremer C, Moore A, Weissleder R (2002a) Detection of lymph node metastases by contrast-enhanced MRI in an experimental model. Magn Reson Med 47(2):292–297

Wunderbaldinger P, Josephson L, Weissleder R (2002b) Crosslinked iron oxides (CLIO): a new platform for the development of targeted MR contrast agents. Acad Radiol 9:S304–S306

Xie H, Wang ZJ, Bao A, Goins B, Phillips WT (2010) In vivo PET imaging and biodistribution of radiolabeled gold nanoshells in rats with tumor xenografts. Int J Pharm 395:324–330

Xie L, Wang G, Zhou H, Zhang F, Guo Z, Liu C, Zhang X, Zhu L (2016) Funcional long circulating single walled carbon nanotubes for fluorescent/photoacoustic imaging-guided enhanced phototherapy. Biomaterials 103:219–228

Xing Y, Zhao J, Conti PS, Chen K (2014) Radiolabeled Nanoparticles for multimodality tumorimaging. Theranostics 4:290–306

Xue S, Wang Y, Wang M, Zhang L, Du X, Gu H, Zhang C (2014) Iodinated oil-loaded, fluorescent mesoporous silica-coated iron oxide nanoparticles for magnetic resonance imaging/computed tomography/fluorescence trimodal imaging. Int J Nanomed 9:2527

Yang H, Zhang J, Tian Q, Hu H, Fang Y, Wu H, Yang S (2010) One-pot synthesis of amphiphilic superparamagnetic Fe-Pt nanoparticles and magnetic resonance imaging in vitro. J Magn Magn Mater 322(8):973–977

Yang K, Wan J, Zhang S, Zhang Y, Lee ST (2011) In vivo pharmacokinetics, long-term biodistribution, and toxicology of PEGylated graphene in mice. ACS Nano 5:516–522

Yong KT (2009) Mn-doped near-infrared quantum dots as multimodal targeted probes for pancreatic cancer imaging. Nanotechnology 20(1):015102

Yu SB, Watson AD (1999) Metal-based X-ray contrast media. Chem Rev 99(9):2353–2377

Zerda A, Zavaleta C, Keren S, Vaithilingam S, Bodapati S, Liu Z, Levi J, Ma TJ, Oralkan O, Cheng Z, Chen X, Dai H, Yakub BTK, Gambhir SS (2008) Carbon nanotubes as photoacoustic molecular imaging agents in living mice. Nat Nanotechnol 3(9):557–562

Zhang WH, Hu XX, Zhang XB (2016) Dye-doped fluorescent silica nanoparticles for live cell and *in vivo* bioimaging. Nanomaterials 6:81